Nonsequential Link Adaptation Using Repetition Codes for Wi-Fi Backscatter Communication

Richard Boateng Nti, Derek Kwaku Pobi Asiedu, Ji-Hoon Yun

Nonsequential Link Adaptation Using Repetition Codes for Wi-Fi Backscatter Communication

Richard Boateng Nti, Derek Kwaku Pobi Asiedu, *Member, IEEE* and Ji-Hoon Yun, *Senior Member, IEEE*

***Abstract*—To enhance the throughput performance and reliability of Wi-Fi backscatter communication, we develop a nonsequential link adaptation scheme using repetition codes and voting to obtain the final decoded bit from repeated bits. To address the estimation of channel conditions from limited transmission results, we convert the packet success rate of one coding scheme into that of another via virtual independent and identically distributed bit errors. The packet success rates that would result in equal expected throughputs of different repetition codes are similarly derived and used as code selection thresholds. We prototype the proposed scheme and, via testbed experiments incorporating commercial Wi-Fi receivers, demonstrate the effectiveness of link adaptation using repetition codes and the throughput gain of the proposed scheme over benchmark schemes.**

***Index Terms*—Wi-Fi backscatter communication, link adaptation, repetition code**

I. Introduction

Wi-Fi backscatter communication, in which a low-cost and low-power tag reflects ambient Wi-Fi signals to transmit its information bits, has been gaining considerable attention due to the popularity of the Wi-Fi standard, which is incorporated into most smart gadgets, and the ubiquity of Wi-Fi networks, which can consequently provide reliably abundant Wi-Fi signals as excitation for tag operation. However, decoding the data bits from backscattered Wi-Fi signals is challenging because a Wi-Fi signal itself exhibits inherent fluctuations due to the typically high peak-to-average power ratio (PAPR) of orthogonal frequency-division multiplexing (OFDM). As the channel gain of a tag decreases, the fluctuations of the Wi-Fi carrier signal begin to overwhelm the pattern of the backscattered signal, resulting in a short communication range.

Many research works on Wi-Fi backscatter communication have focused on increasing the reliability of communication in the face of such fluctuations in the Wi-Fi carrier signal as well as varying channel conditions. In some studies, the frequency shift technique has been employed [1], [2] to move the backscattered signal into a frequency channel other than that of the carrier signal. In [2], Reed–Solomon codes were used for forward error correction (FEC) to enhance transmission reliability. Reliable decoding algorithms have been proposed that utilize unique signal patterns resulting from the smoothing of Wi-Fi signals [3] and multiple filters to exclude undesired interference from Wi-Fi carrier signals [4]. Other approaches include the combining of temporally repeated signals [5] and spectro-temporal combining to additionally combat incumbent interference in frequency-shifted channels [6].

Link adaptation (LA) has been adopted in most de facto wireless communication systems to achieve not only high throughput but also reliable communication by adaptively modifying the modulation/coding schemes—and thus, the transmission bit rates—in response to varying channel conditions. This approach is also expected to be beneficial for Wi-Fi backscatter communication. To permit the realization of LA in Wi-Fi backscatter communication, a tag must first support multiple transmission bit rates. Moreover, it is essential for this implementation of multiple transmission bit rates to be affordable considering the low-cost constraint of such tags.

For LA, a tag must also be able to (1) estimate the current channel conditions and (2) switch to an optimal modulation/coding scheme accordingly. Since no commercial Wi-Fi transceivers provide the channel-related information of backscattered signals, the current channel conditions of a tag must instead be estimated based on its packet transmission results. For this purpose, two representative classes of methods have been considered: *counting-based* and *statistics-based* methods. Counting-based schemes—including automatic rate fallback (ARF) [7] and many other variants for wireless local area networks (WLANs) as well as variants for backscatter networks [5], [6]—involve estimating the channel conditions for the current bit rate based on the most recent numbers of transmission successes and failures at the current bit rate. Statistics-based schemes—including Minstrel [8] and its variants for WLANs—rely on measuring the statistics of the transmission results for all bit rates and determining the current channel conditions based on the statistical throughput at each rate.

The bit rate selection schemes for a Wi-Fi backscatter tag can be classified into the following two types:

- *Sequential selection*: The bit rate is changed to the next lower/higher rate. Counting-based schemes are associated with this type of selection.
- *Nonsequential selection*: The best bit rate is immediately selected from all rates, typically based on the statistics of the associated transmission results.

Nonsequential selection enables more responsive adaptation to varying channel conditions than sequential selection by allowing the immediate use of any bit rate, but the challenge associated with it is that the performance under all bit rates must be estimated for the current channel conditions. If only

Richard Boateng Nti, Derek Kwaku Pobi Asiedu and Ji-Hoon Yun are with the Department of Electrical and Information Engineering, Seoul National University of Science and Technology, Seoul 01811, Republic of Korea.

Corresponding author: Ji-Hoon Yun (email: jhyun@seoultech.ac.kr).

This study was financially supported in part by a grant from the Institute of Information Communications Technology Planning & Evaluation (IITP) funded by the Korean Government (MSIT) (No. 2017-0-00650), in part by a grant from the National Research Foundation of Korea (NRF) funded by the Korean government (MSIT) (No. 2020R1F1A1077402) and in part by the Seoul National University of Science and Technology.

This article has been accepted for publication in IEEE Transactions on Vehicular Technology. This is the author's version which has not been fully edited and content may change prior to final publication. Citation information: DOI 10.1109/TVT.2024.3352084

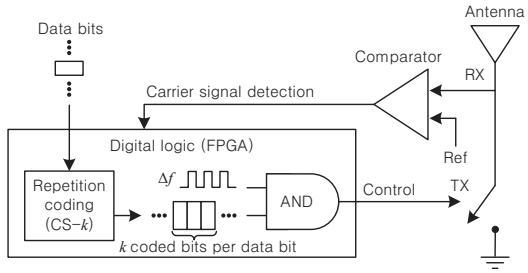

(a) Tag system

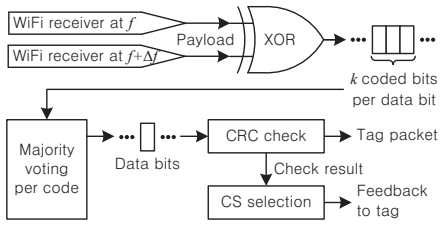

(b) Receiver system

Fig. 1. Processing flow of the proposed tag and receiver systems with repetition coding.

a limited set of bit rates are used for a certain period of time, then the transmission statistics for other rates become outdated, thus resulting in inaccurate performance estimation for less-used rates.

In this paper, we develop a nonsequential LA scheme using repetition codes for Wi-Fi backscatter communication and demonstrate its feasibility and advantages via prototyping and testbed experiments using commodity Wi-Fi receivers. Repetition coding is a simple way to increase communication reliability by repeating an information bit without substantially changing the existing bit synthesis pipeline; thus, it is affordable for backscatter tags and can also be combined with other transmission schemes of diverse types. We use simple majority voting to obtain the final decoded bit from the repeated bits. To address the challenge of estimating the channel conditions from limited transmission results, we convert the packet success rate of one coding scheme into that of another via virtual independent and identically distributed (i.i.d.) bit errors, which is made possible by the consistent structure of repetition codes of different lengths. Then, the channel conditions to be used for code selection can be obtained by integrating the packet success rates under different coding schemes, thus ensuring up-to-date estimation. The packet success rates that would result in equal expected throughputs of different repetition codes are similarly derived and used for selection of a repetition code. Our approach enables a direct and responsive transition to the best repetition code without traversing through all intermediate codes, i.e., nonsequential selection, which is well-suited for our target scenario leveraging multiple repetition codes for finer adaptability to diverse channel conditions. We demonstrate via testbed experiments that the proposed scheme outperforms benchmark schemes under various communication conditions, achieving up to 3.5× throughput under some conditions.

II. Tag and Receiver System Model Using Repetition Codes

The communication system under consideration consists of a Wi-Fi transmitter acting as a carrier source, a backscatter tag, and a receiver. Fig. 1 shows the block diagrams of our prototype tag and receiver designs. Once the tag detects a Wi-Fi signal above a certain reference level, the transmission procedure of the digital logic (field-programmable gate array, FPGA) is triggered. The data bits first pass through the coding block. We use CS-k to denote the coding scheme (CS) using a repetition code of length k. In CS-k, one information bit is represented by k coded bits that have the same bit value as the information bit. The output bits from the coding block are then input into an AND gate with a clock signal at a frequency of Δf, which is the amount by which the frequency is to be shifted from the carrier signal's frequency. The output signal of the AND gate is then input into the control port of an RF switch placed between the antenna and ground to control its state between reflection and absorption to perform codeword translation of the Wi-Fi OFDM signal.

The receiver receives two backscattered Wi-Fi signals, one in the carrier-signal channel and the other in the shifted channel, and performs an XOR operation on the two signals, as proposed in [1], to obtain the coded bits. Finally, the coded bits are decoded into data bits through majority voting. If CS-k is used for the coded bits, then the voting mechanism will select the majority bit value among these k bits. To avoid the ambiguous case in which equal numbers of bit values are obtained for both one and zero, we use only odd values for k. For CS-1, there is no code repetition, and an error of a coded bit is equivalent to an error of an information bit.

III. Link Adaptation Using Repetition Codes

A trade-off exists between reliability and efficiency when selecting a repetition code. For CS-k, if more than half of the k coded bits are corrupted, a bit error of the corresponding information bit is produced. Therefore, as k increases, the bit error rate (BER) generally decreases. However, as k increases, k times the airtime must be used to transmit the same number of information bits. This implies that k must be adaptively selected such that under good channel conditions, when the probability of error is low, a small k will be used to reduce airtime, while under poor channel conditions, a larger k will be used to enhance the reliability of transmission, seeking the highest throughput in both cases. That is, the purpose of adaptation is to select the best CS-k^* that will achieve the highest expected throughput from among all available CSs; this is expressed as

$$k^* = \arg\max_k T_k, \tag{1}$$

where the normalized expected throughput T_k under CS-k is given by

$$T_k = \frac{p_{s,k}}{k}, \tag{2}$$

where $p_{s,k}$ is the packet success rate of CS-k.

In the following, we describe the framework of the proposed LA scheme and the detailed threshold configuration; its

Algorithm 1 Link adaptation using repetition codes

k^*: CS currently in use
R_k: Transmission result for a tag packet using CS-k; equal to 1 if the transmission succeeds, 0 otherwise
α_1, α_2: Weights for the EWMA calculation
for each tag-packet transmission **do**
  $\bar{p}_{s,k^*}[t] \leftarrow \alpha_1 R_{k^*}[t] + (1-\alpha_1)\bar{p}_{s,k^*}[t-1]$
  Obtain $p_{b,k^*}[t]$ from $\bar{p}_{s,k^*}[t]$ using Eq. (5)
  Obtain $p_{b,1}[t]$ from p_{b,k^*} using Eq. (6)
  Obtain the equivalent $\bar{p}^{eq}_{s,1}[t]$ from $p_{b,1}$ using Eq. (4)
  $\bar{p}_{s,1}[t] \leftarrow \alpha_2 \bar{p}^{eq}_{s,1}[t] + (1-\alpha_2)\bar{p}_{s,1}[t-1]$
  for $k = 1, 3, 5, \ldots$ **do**
    if $\bar{p}_{s,1}[t] \leq \Pr\{p_{s,1}|T_k = T_{k+2}\}$ **then**
      $k^* \leftarrow k$
    end if
  end for
  $t \leftarrow t+1$
end for

pseudocode is also given in Algorithm 1. Regarding notation, we denote the value of the variable x for packet t by $x[t]$.

A. Algorithm Framework

The current channel conditions are first represented by the exponentially weighted moving average (EWMA) of the packet success rate under each CS, which we denote by $\bar{p}_{s,k}$ for CS-k and obtain as follows:

$$\bar{p}_{s,k}[t] \leftarrow \alpha_1 R_k[t] + (1-\alpha_1)\bar{p}_{s,k}[t-1], \tag{3}$$

where $R_k = 1$ if a transmission succeeds and $R_k = 0$ otherwise, while α_1 is the weight for the EWMA calculation. To integrate the transmission results for all CSs into a single indicator, i.e., $\bar{p}_{s,1}$, we calculate the equivalent packet success rate of CS-1 corresponding to $\bar{p}_{s,k}$, which we denote by $\bar{p}^{eq}_{s,1}$. For this purpose, we introduce an intermediary variable $p_{b,k}$, which is interpreted as a virtual i.i.d. BER of CS-k. It should be noted that $p_{b,k}$ is not exactly the actual BER but rather an imaginary variable used to relate the success rates under different CSs. Let L be the number of coded bits of a tag packet within a Wi-Fi frame. We can express $p_{s,k}$ in terms of the i.i.d. BER $p_{b,k}$ as follows:

$$p_{s,k} = (1-p_{b,k})^{\lfloor L/k \rfloor}, \tag{4}$$

from which $p_{b,k}$ is obtained as

$$p_{b,k} = 1 - (p_{s,k})^{1/\lfloor L/k \rfloor}. \tag{5}$$

When CS-k is used, successful decoding of an information bit is achieved if at least $\lceil k/2 \rceil$ coded bits are successfully decoded. Since the error rate of the coded bits is the same as the BER of CS-1, i.e., $p_{b,1}$, the decoding success probability for an information bit under CS-k can be obtained in terms of $p_{b,1}$ as follows:

$$\sum_{j=\lceil k/2 \rceil}^{k} \binom{k}{j} (1-p_{b,1})^j p_{b,1}^{k-j} = 1 - p_{b,k} = (p_{s,k})^{1/\lfloor L/k \rfloor}, \tag{6}$$

where the second equality arises from the application of Eq. (5). Once $\bar{p}_{s,k}$ is known from Eq. (3), it can be applied in Eq. (6), and a numerical solver can be used to obtain the corresponding $p_{b,1}$, which we thus denote by $\bar{p}^{eq}_{b,1}$. We obtain $\bar{p}^{eq}_{s,1}$ by applying $\bar{p}^{eq}_{b,1}$ in Eq. (4). Then, by applying the EWMA calculation to $\bar{p}^{eq}_{s,1}$ with a weight α_2 assigned to the previous value of $\bar{p}_{s,1}$, we obtain an updated $\bar{p}_{s,1}$ that finally represents the current channel conditions.

To select the CS that achieves the highest expected throughput, we use a threshold $\Pr\{p_{s,1}|T_k = T_{k+2}\}$ for each k (obtained as described in the next subsection), which is the success rate $p_{s,1}$ obtained when CS-k and CS-$(k+2)$ achieve equal throughput. Note that as the channel conditions improve, a CS with a shorter length becomes more beneficial in terms of throughput. Therefore, if $\bar{p}_{s,1}$ is lower than $\Pr\{p_{s,1}|T_k = T_{k+2}\}$, the current channel conditions are considered sufficiently good to yield $T_k > T_{k+2}$, and thus, it is better to use CS-k. Conversely, if $\bar{p}_{s,1}$ is higher than $\Pr\{p_{s,1}|T_k = T_{k+2}\}$, then $T_k < T_{k+2}$, and it is better to use CS-$(k+2)$. Accordingly, the CS to be used next is determined as

$$k^* \leftarrow \begin{cases} k & \text{if } \bar{p}_{s,1} \leq \Pr\{p_{s,1}|T_k = T_{k+2}\} \\ k+2 & \text{if } \bar{p}_{s,1} \geq \Pr\{p_{s,1}|T_k = T_{k+2}\} \end{cases}. \tag{7}$$

Thus, once we have obtained the thresholds $\Pr\{p_{s,1}|T_k = T_{k+2}\}$ for all k, we can determine the CS that achieves the highest throughput based on $\bar{p}_{s,1}$. We obtain these thresholds as described in the following subsection.

B. Threshold Configuration

Let $p^*_{s,k}$ and $p^*_{s,k+2}$ be the packet success rates of CS-k and CS-$(k+2)$, respectively, when the equality $T_k = T_{k+2}$ holds. Then, we have

$$p^*_{s,k+2} = \frac{k+2}{k} p^*_{s,k}. \tag{8}$$

The virtual i.i.d. BERs $p^*_{b,k}$ and $p^*_{b,k+2}$ corresponding to $p^*_{s,k}$ and $p^*_{s,k+2}$, respectively, are obtained using Eq. (5). Substituting them into Eq. (8) yields

$$\begin{aligned} p^*_{b,k+2} &= 1 - (p^*_{s,k+2})^{1/\lfloor L/(k+2) \rfloor} \\ &= 1 - (\tfrac{k+2}{k} p^*_{s,k})^{1/\lfloor L/(k+2) \rfloor}. \end{aligned} \tag{9}$$

Let the BER of CS-1 corresponding to $p^*_{s,k}$ be denoted by $p^*_{b,1}$; then, Eq. (6) can be rewritten as

$$p^*_{s,k} = \left(\sum_{j=\lceil k/2 \rceil}^{k} \binom{k}{j} (1-p^*_{b,1})^j (p^*_{b,1})^{k-j} \right)^{\lfloor L/k \rfloor}. \tag{10}$$

After replacing k with $k+2$ in Eq. (6), we substitute $p^*_{s,k+2}$ with $p^*_{s,k}$ based on Eq. (9) and obtain

$$p^*_{s,k} = \beta_1 \left(\sum_{j=\lceil (k+2)/2 \rceil}^{k+2} \binom{k+2}{j} (1-p^*_{b,1})^j (p^*_{b,1})^{k+2-j} \right)^{\beta_2}, \tag{11}$$

where $\beta_1 = \dfrac{k}{k+2}$ and $\beta_2 = \lfloor L/(k+2) \rfloor$. Eqs. (10) and (11) can be solved with respect to $p^*_{b,1}$ using a numerical solver. Finally, $\Pr\{p_{s,1}|T_k = T_{k+2}\}$ is obtained from Eq. (4) as $(1-$

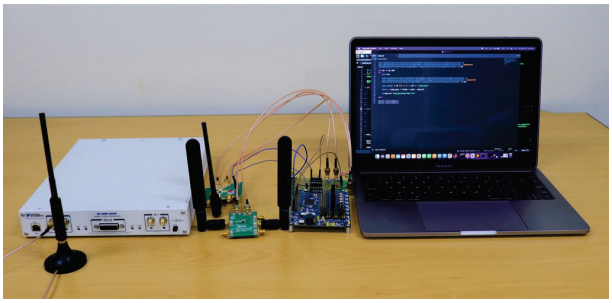

Fig. 2. Tag hardware prototype and testbed configuration.

$p^*_{b,1})^L$. By considering other CSs in Eq. (8), we can obtain the thresholds for all k.

IV. Performance Evaluation

In this section, we evaluate the proposed scheme based on testbed experiments.

A. Experimental Setup

Fig. 2 shows our tag hardware prototype and testbed configuration. An Ettus Universal Software Radio Peripheral (USRP X310) acts as a Wi-Fi transmitter (TX) to generate Wi-Fi (IEEE 802.11g OFDM) carrier signals at a rate of 6 Mbps The backscatter tag consists of a carrier-signal detection circuit equipped with an AD8313 RF meter (Analog Devices) and an LM393 comparator (Texas Instruments) with a reference voltage of 1.1 V, an AGLN250 FPGA board (Microsemi) for control signal generation with a frequency shift (Δf) of 20 MHz, and an ADG902 RF switch (Analog Devices) to reflect/absorb Wi-Fi signals. The receiving device (RX) is a MacBook Pro with a built-in Wi-Fi transceiver, where the backscattered data bits are decoded from the received Wi-Fi frames. In each Wi-Fi frame, 64 coded bits are sent, i.e., L = 64. Each packet transmitted by the backscatter tag consists of a 4-bit header, a payload and a 4-bit cyclic redundancy check. For the EWMA calculation, we set $\alpha_1 = \alpha_2 = 0.7$. Three cases of different TX-to-tag distances are considered: 0.5, 1, and 2 m. For each TX-to-tag distance, the receiver is also placed at different distances from the TX and tag, with tag-to-RX distances of 0.5, 1, 5, and 9 m.

We consider counting (Cnt)-based and statistics (Stat)-based schemes as benchmarks. For the Cnt-based scheme, we consider two pairs—(4, 2) and (3, 3)—of numbers of consecutive transmission successes and failures that trigger a decrease in the CS length to the next lower one and an increase in the CS length to the next higher one, respectively. In the Stat-based scheme, the average packet success rate of each CS ($\bar{p}_{s,k}$ for CS-k) is measured in the same manner as in the proposed scheme. Then, the expected throughput (T_k) of each CS is calculated, and either the CS with the highest expected throughput or, with an exploration probability of 10%, a random CS is selected.

B. Evaluation Results

Fig. 3 shows the throughput performance of the considered LA and fixed CS schemes for varying tag-to-RX distances. Under good channel conditions (short TX-to-tag and tag-to-RX distances), CSs with short lengths perform better than those with longer lengths. However, as the tag-to-RX distance increases, the throughput of CSs with shorter lengths decreases more rapidly. The trend of decreasing throughput for CSs with short lengths with an increasing tag-to-RX distance becomes more severe as the TX-to-tag distance increases. For the TX-to-tag distance of 1 m (Fig. 3(b)), CS-1 performs worse than CS-5 for tag-to-RX distances over 3 m and becomes the worst among all CSs for tag-to-RX distances over 5 m. For the TX-to-tag distance of 2 m (Fig. 3(c)), CS-1 is always the worst, CS-3 is the best up to a tag-to-RX distance of 3 m, and CS-5 and CS-7 become better than CS-3 for tag-to-RX distances over 4 m. These results for the fixed CS cases clearly show that (1) using repetition coding enhances throughput performance under poor channel conditions and (2) an adaptation algorithm is essential for varying channel conditions.

Fig. 3 also demonstrates that the proposed scheme adaptively selects the best (or near-best) CS and outperforms the benchmark schemes. This is first observed at a tag-to-RX distance of 9 m in Fig. 3(a), where CS-1 is no longer the best CS, but the proposed scheme avoids suffering the throughput decrease of CS-1 by switching to another CS. The reason why the proposed scheme achieves higher throughput than any single CS on average is that the best CS changes over time, and the CS changes accordingly under the proposed scheme. In Fig. 3(b), CS-3 is the best option on average for tag-to-RX distances from 3 to 8 m, and the proposed scheme is shown to successfully follow the throughput curve of CS-3 at tag-to-RX distances over 5 m, while the benchmarks fail to do so. Thus, the proposed scheme always outperforms them, with up to 3.5× throughput compared to the Cnt-based-(4, 2) scheme at 1 m. The proposed scheme, however, has a slightly lower throughput than CS-3 at a tag-to-RX distance of 5 m and compared to CS-5 at a tag-to-RX distance of 9 m, since it tends to use a shorter CS length than the optimal one for these channel conditions, as shown in Fig. 5(b).

Finally, in the worst-channel-condition scenario shown in Fig. 3(c), the expected performance of the proposed scheme is no different from the previous observations, either following the best CS or attaining even higher throughput. The benchmark schemes achieve significantly lower performance than the proposed scheme up to a tag-to-RX distance of 4 m, although they successfully select the best CS at tag-to-RX distances over 5 m. Fig. 3(c) shows nearly overlapping curves of Cnt-based-(4, 2) and -(3, 3). This is because the Cnt-based scheme predominantly uses CS-7 in both configuration cases as illustrated in Fig. 6(c). The cumulative distribution functions (CDFs) of throughput samples shown in Fig. 4 (each sample is a measure for 20 consecutive tag packets) demonstrate that the proposed scheme consistently outperforms the other schemes across all samples.

To investigate the prediction accuracy, we show the CDFs of the gaps between the optimal CS (the one with the shortest length that results in no errors) and the ones selected by the proposed and benchmark schemes in Fig. 5. The gap with respect to the optimal CS is defined as the difference between the lengths of the two CSs; if the gap is positive

This article has been accepted for publication in IEEE Transactions on Vehicular Technology. This is the author's version which has not been fully edited and content may change prior to final publication. Citation information: DOI 10.1109/TVT.2024.3352084

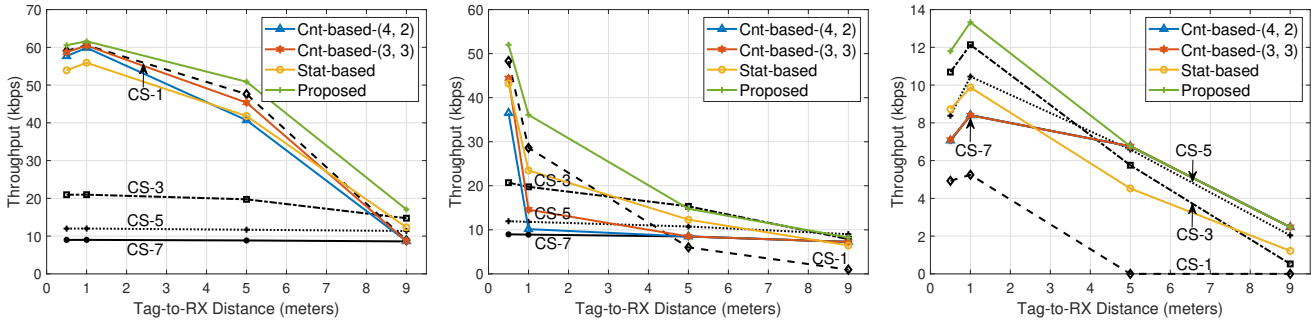

(a) TX-to-tag distance: 0.5 m (b) TX-to-tag distance: 1 m (c) TX-to-tag distance: 2 m

Fig. 3. Throughput performance of the LA schemes for varying tag-to-RX distances

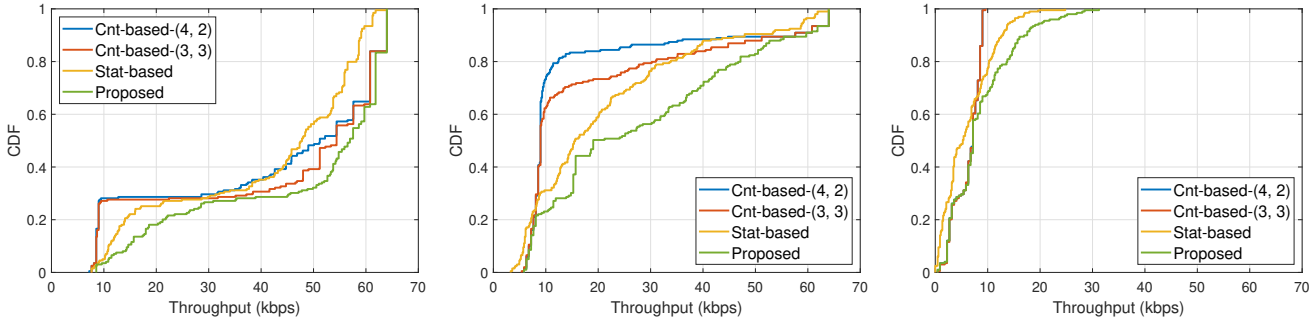

(a) TX-to-tag distance: 0.5 m (b) TX-to-tag distance: 1 m (c) TX-to-tag distance: 2 m

Fig. 4. CDF of throughput performance of the LA schemes for varying tag-to-RX distances.

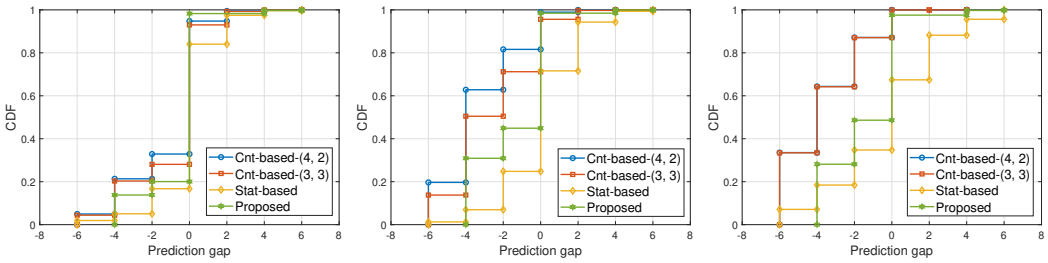

(a) TX-to-tag distance: 0.5 m (b) TX-to-tag distance: 1 m (c) TX-to-tag distance: 2 m

Fig. 5. CS selection accuracy.

(negative), then the CS selected by the corresponding scheme has a longer (shorter) length than the optimum. The subfigure corresponding to the TX-to-tag distance of 0.5 m (Fig. 5(a)) shows that the selection results of the proposed scheme match the optimal choices for approximately 80% of the samples, whereas 60∼65% of the selections are optimal under the Cnt-based and Stat-based schemes. For the other two TX-to-tag distance cases (Fig. 5(b) and (c)), the proposed scheme matches the optimal choices for approximately 50% of the samples, whereas 40% and 30% of the selections are optimal under the Cnt-based and Stat-based schemes, respectively.

Fig. 4 shows the CS distributions of the LA schemes along with the packet error rates (PERs). The Cnt-based scheme shows conservative behavior, quickly ramping to CS-7 even under moderate channel conditions for both threshold configuration cases. The proposed scheme mostly selects CS-1 under good channel conditions and increases the usage frequency of CS-7 as the channel conditions worsen. Thus, the proposed scheme achieves higher throughput than the Cnt-based scheme, although the Cnt-based scheme achieves similar or slightly lower PERs than the proposed scheme. The Stat-based scheme uses diverse CSs under all considered conditions and results in the highest PERs among the compared schemes.

To assess the impact of external interference on performance within a controlled environment, we emulate interference signals overlaid onto a signal trace. These interference signals have a duration of 1 ms and their presence is regulated by a specified probability denoted as p. The tag-to-RX distance is fixed at 0.5 m. The throughput results for varying p are presented in Fig. 7. As p increases, the throughput of all schemes experiences a significant decrease. However, the proposed scheme consistently maintains the highest throughput performance among all schemes, indicating its superior adaptability even in the presence of external interference.

Fig. 8 shows the throughput performance across various (α_1, α_2) values. We set $\alpha_1 = \alpha_2$ for simplicity. The results in the figure consistently demonstrate that the configuration with ($\alpha_1 = \alpha_2$) = 0.7 employed throughout our experiments outperforms the other configuration settings due to its effective balance between smoothing and responsiveness.

This article has been accepted for publication in IEEE Transactions on Vehicular Technology. This is the author's version which has not been fully edited and content may change prior to final publication. Citation information: DOI 10.1109/TVT.2024.3352084

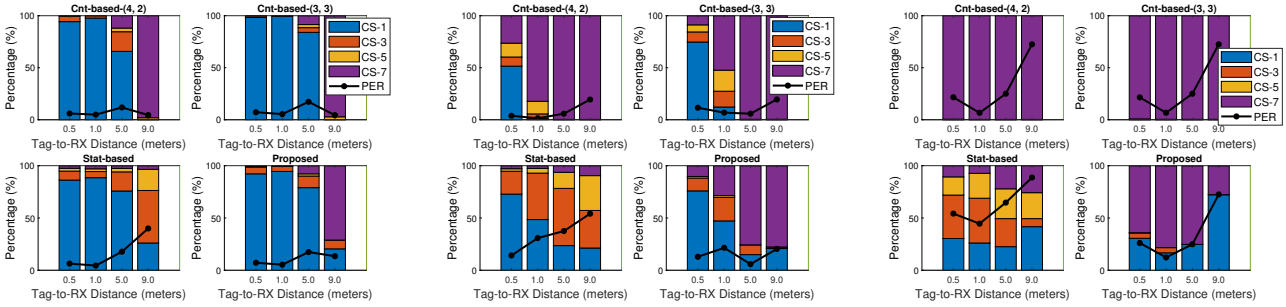

(a) TX-to-tag distance: 0.5 m (b) TX-to-tag distance: 1 m (c) TX-to-tag distance: 2 m

Fig. 6. CS distribution breakdowns of the LA schemes.

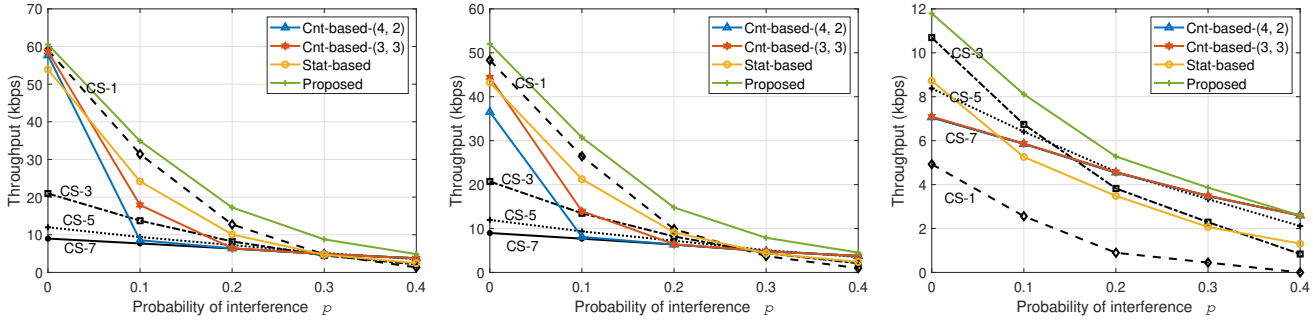

(a) TX-to-tag distance: 0.5 m (b) TX-to-tag distance: 1 m (c) TX-to-tag distance: 2 m

Fig. 7. Impact of external interference on throughput performance for the LA schemes with various probabilities of interference.

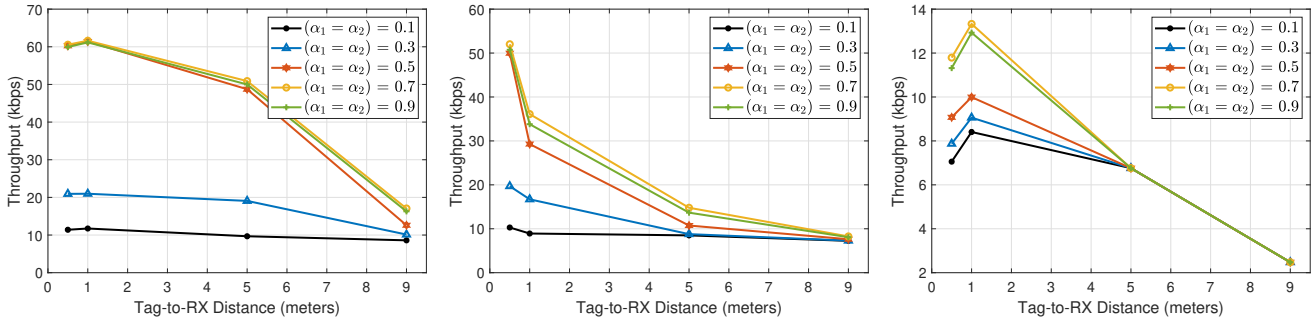

(a) TX-to-tag distance: 0.5 m (b) TX-to-tag distance: 1 m (c) TX-to-tag distance: 2 m

Fig. 8. Impact of α_1 and α_2 on throughput performance for the proposed LA scheme.

V. Conclusion

We have developed an LA scheme employing repetition codes for Wi-Fi backscatter communication. The proposed scheme integrates the packet success rates from different coding schemes for channel condition estimation and selects the optimal code using calculated thresholds. Testbed experiments with commodity Wi-Fi receivers have demonstrated the superior reliability and adaptability of the proposed scheme over benchmark schemes across diverse communication conditions. Future studies will involve extending the solution to diverse environments, including multiple tags and carrier sources, and integrating experiments with a network simulator for complex large-scale interference scenarios.

References

[1] P. Zhang, C. Josephson, D. Bharadia, and S. Katti, "FreeRider: Backscatter communication using commodity radios," in *Proc. ACM CoNEXT*, Seoul/Incheon, South Korea, Nov. 2017.

[2] X. He, W. Jiang, M. Cheng, X. Zhou, P. Yang, and B. Kurkoski, "Guardrider: Reliable WiFi backscatter using reed-Solomon codes with QoS guarantee," in *Proc. IEEE/ACM IWQoS*, Jun. 2020.

[3] H. Hwang, J.-H. Lim, J.-H. Yun, and B. J. Jeong, "Pattern-based decoding for Wi-Fi backscatter communication of passive sensors," *Sensors*, vol. 19, no. 5, Mar. 2019.

[4] R. B. Nti and J.-H. Yun, "Multi-filter decoding in WiFi backscatter communication," *Sensors*, vol. 21, no. 4, Feb. 2021.

[5] H. Hwang and J.-H. Yun, "Adaptive transmission repetition and combining in bistatic WiFi backscatter communications," *IEEE Access*, vol. 8, pp. 55 023–55 031, 2020.

[6] H. Hwang, R. B. Nti, and J.-H. Yun, "Spectro-temporal combining in bistate WiFi backscatter communication with frequency shift," *IEEE Access*, vol. 9, pp. 113 735–113 747, 2021.

[7] A. Kamerman and L. Monteban, "WaveLAN-II: a high-performance wireless LAN for the unlicensed band," *Bell Labs Technical Journal*, vol. 2, no. 3, pp. 118–133, 2002.

[8] D. Xia, J. Hart, and Q. Fu, "Evaluation of the Minstrel rate adaptation algorithm in IEEE 802.11g WLANs," in *Proc. IEEE ICC*, Budapest, Hungary, Nov. 2013.